

RESEARCH

Open Access



Engineering quorum sensing-based genetic circuits enhances growth and productivity robustness of industrial *E. coli* at low pH

Xiaofang Yan¹, Anqi Bu¹, Yanfei Yuan¹, Xin Zhang¹, Zhanglin Lin^{1,2*} and Xiaofeng Yang^{1*}

Abstract

Background Microbial organisms hold significant potential for converting renewable substrates into valuable chemicals. Low pH fermentation in industrial settings offers key advantages, including reduced neutralizer usage and decreased wastewater generation, particularly in the production of amino acids and organic acids. Engineering acid-tolerant strains represents a viable strategy to enhance productivity in acidic environments. Synthetic biology provides dynamic regulatory tools, such as gene circuits, facilitating precise expression of acid resistance (AR) modules in a just-in-time and just-enough manner.

Results In this study, we aimed to enhance the robustness and productivity of *Escherichia coli*, a workhorse for amino acid and organic acid production, in industrial fermentation under mild acidic conditions. We employed an Esa-type quorum sensing circuit to dynamically regulate the expression of an AR module (DsrA-Hfq) in a just-in-time and just-enough manner. Through careful engineering of the critical promoter P_{esaS} and stepwise evaluation, we developed an optimal $\text{Esa-}P_{\text{BD}}(\text{L})$ circuit that conferred upon an industrial *E. coli* strain SCECL3 comparable lysine productivity and enhanced yield at pH 5.5 compared to the parent strain at pH 6.8.

Conclusions This study exemplifies the practical application of gene circuits in industrial environments, which present challenges far beyond those of well-controlled laboratory conditions.

Keywords Acid resistance, Gene circuit, Quorum sensing, Lysine production, *Escherichia coli*

Background

Microbial biomanufacturing has the potential to utilize renewable substrates to produce value-added chemicals in a sustainable and environment-friendly manner, and bio-manufactured products are expected to replace approximately 35% of petroleum and coal-based chemical products until 2030 [1]. During industrial bioprocesses, microbes often encounter multiple stresses such as heat, acid, oxidative, and osmotic stresses, with acid stress being a significant concern [2–4]. The accumulation of acidic metabolic products lowers the pH of fermentation liquor, which damage cell growth and productivity [5–7]. While adding bases during fed-batch fermentation

*Correspondence:

Zhanglin Lin
zhanglinlin@gdut.edu.cn
Xiaofeng Yang
biyangxf@scut.edu.cn

¹School of Biology and Biological Engineering, South China University of Technology, Guangzhou 510006, Guangdong, China

²Present address: School of Biomedicine, Guangdong University of Technology, Guangzhou 510006, Guangdong, China



© The Author(s) 2024. **Open Access** This article is licensed under a Creative Commons Attribution-NonCommercial-NoDerivatives 4.0 International License, which permits any non-commercial use, sharing, distribution and reproduction in any medium or format, as long as you give appropriate credit to the original author(s) and the source, provide a link to the Creative Commons licence, and indicate if you modified the licensed material. You do not have permission under this licence to share adapted material derived from this article or parts of it. The images or other third party material in this article are included in the article's Creative Commons licence, unless indicated otherwise in a credit line to the material. If material is not included in the article's Creative Commons licence and your intended use is not permitted by statutory regulation or exceeds the permitted use, you will need to obtain permission directly from the copyright holder. To view a copy of this licence, visit <http://creativecommons.org/licenses/by-nc-nd/4.0/>.

can alleviate acid stress, it increases costs and generates excess waste streams [3, 7]. Thus, the engineering of cellular resistance against acid stress to improve the production robustness has been a long-standing critical challenge for bioprocess economics.

In *E. coli*, acid resistance (AR) is a complex phenotype governed by a multi-layer hierarchical network [8] through various mechanisms, including physiological adaptations, metabolic responses, and proton-consuming reactions [9]. Currently, two main strategies have been used to enhance the acid resistance for microbial cells: (1) manipulating AR-related global transcription regulators [10] such as IrrE [11], H-NS (histone-like nucleoid structuring factor) [12], and CRP (cAMP receptor protein) [13]; (2) developing synthetic acid stress-tolerance modules controlled by acid-responsive promoters [14]. The latter modules encompass various genes involved in multiple AR mechanisms, including proton-consumption, protein protection, and ROS scavenging. However, the industrial application of transcription regulator manipulation is constrained by the inefficient resource consumption due to the continuous and simultaneous perturbation of hundreds of genes throughout the cell cycle [10, 15]. For synthetic acid stress-tolerance modules, our study showed one such module successfully maintained the productivity of an industrial *E. coli* strain at pH 6.0 to a level comparable to that of at pH 6.8, but it failed at lower pH condition (e.g. pH 5.5), suggesting the limited capacities of these modules in conferring stress tolerance.

Over the years, it has been found that *E. coli* is sensitive to acid stress in the exponential phase but becomes tolerant in the stationary phase [16–18], and that the over-expression of AR-related genes in the exponential phase is the main contributor for the acid tolerant strains [12, 19]. We therefore sought to overcome these limitations by applying a gene circuit to dynamically regulate the expression of AR-related genes. One particularly interesting target would be the general stress sigma factor RpoS [9, 19–21]. RpoS plays a crucial role as a mediator between the AR-related global regulators and the specific stress response genes, either directly or indirectly [22–24]. The translation of *rpoS* mRNA can be activated by three small RNA (sRNAs), i.e., DsrA, ArcZ, and RprA, either individually or in combination [20], in the presence of the RNA chaperone Hfq. Our recent work has shown that co-expression of DsrA and Hfq can significantly enhance the acid growth performance of *E. coli*, and the optimal DsrA-Hfq module variant can increase the biomass of *E. coli* at pH 4.5 by 50~70% [19]. However, the module failed to improve the productivity of the industrial strain, likely because the expression of this module was not coordinated with the cell growth and production [25–27].

In this study, we aimed to devise an “ON to OFF” genetic circuit that enhances the expression of the DsrA-Hfq module during the exponential phase, but shuts down the expression during the stationary phase. To date, only a handful of gene switches or circuits can exhibit an “ON to OFF” output pattern, like riboswitches [28], robust perfect adaptation (RPA) circuits [29], and quorum sensing (QS) circuits [26, 30–32]. These circuits are typically employed for executing logical operations, controlling pattern formation, or regulating metabolic flux, often at theoretical or laboratory scales. However, their utilization in industrial fermentation processes has yet to be realized, likely due to the intricate nature of cells within an industrial environment, encompassing culture media and operational conditions [33, 34]. We selected the QS circuit [25] as it does not require an externally supplied inducer, but instead depends on an autoinducer, e.g., N-Acyl homoserine lactone (AHL). An AHL-mediated QS circuit conceptually contains three units: activation, inhibition, and response units [26, 35]. Figure 1A gives a brief description of our circuit design: (1) The activation unit produces the transcriptional regulator EsaRI70V [25, 36], the inhibition unit produces the AHL synthase EsaI, and the response unit expresses the reporter module (sfGFP or mCherry) or the AR module (DsrA-Hfq); (2) In the absence of AHL, the EsaRI70V dimer binds to the P_{esaS} promoter, and activates the expression of the reporter module or the AR module. As the cell grows, the AHL accumulates and competitively binds to the EsaRI70V dimer, which disrupts its association with the P_{esaS} promoter and deactivate the expression of the AR module. Therefore, this circuit (hereinafter referred to as the Esa- P_{esaS} circuit) effectively suppresses the gene expression of the AR module in response to increasing cell density.

Here, we discovered that the P_{esaS} promoter is also acid-responsive, thereby interfering with its quorum sensing function under acidic conditions. We systematically engineered the P_{esaS} promoter, effectively uncoupling this low-pH crosstalk and ensuring its exclusive responsiveness to cell density. The optimized Esa- P_{esaS} circuit conferred an industrial *E. coli* strain with lysine productivity at pH 5.5 comparable to that of the parent strain at neutral in fed-batch fermentation. This showcases the utility of gene circuits in bioprocesses to bolster the acid tolerance and productivity resilience of industrial strains. Additionally, this approach shows promise for addressing various stress-related challenges across diverse applications.

Results

Construction and characterization of the Esa- P_{esaS} circuit

As shown in Fig. 1A, we constructed and characterized the Esa- P_{esaS} circuit in the *E. coli* DH10B strain with a

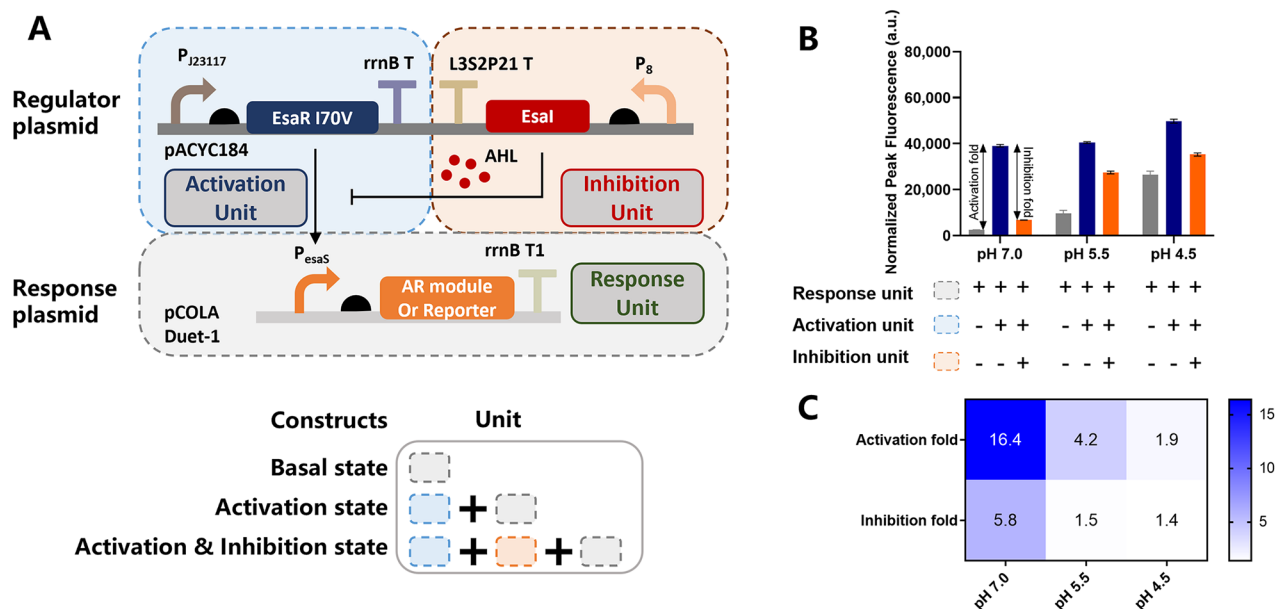


Fig. 1 Design and characterization of the Esa- P_{esaS} circuit. **(A)** Schematic diagram of the Esa- P_{esaS} circuit. The Esa- P_{esaS} circuit was constructed in a dual-plasmid system. The activation unit and the inhibition unit were placed on pACYC184 plasmid, and the response unit was put on pCOLADuet-1 plasmid. The basal state was measured from strain harboring only the response unit. The activation state was measured from strain harboring the activation unit and response unit. The activation & inhibition state was measured from strain harboring the activation unit, the inhibition unit, and the response unit. **(B)** The normalized peak fluorescence in three states of the Esa- P_{esaS} circuit in LBG medium (LB medium with 2% glucose) with different pH conditions (pH 7.0, pH 5.5, and pH 4.5). mCherry was used as reporter here to conduct continuous fluorescence measurements, and the fluorescence was normalized by OD_{600} . The normalized peak fluorescence in three states were used to calculate the activation fold and inhibition fold. The activation fold was defined as the ratio of the normalized peak fluorescence in the activation state to that in the basal state. The inhibition fold was defined as the ratio of the normalized peak fluorescence in the activation state to that in the activation & inhibition state. **(C)** The activation folds and inhibition folds of the Esa- P_{esaS} circuit at pH 7.0, pH 5.5, and pH 4.5. Data are presented as mean \pm s.d. of three replicates

dual-plasmid system, which comprises of a regulator plasmid carrying the activation/inhibition units on the pACYC184 backbone, and a response plasmid carrying the response unit on the pCOLADuet-1 backbone (refer to the “Gene circuit construction” subsection in Methods and Materials) [25, 35–37]. The PJ23117 promoter was selected from seven constitutive promoters [38] to express EsaRI70V in the activation unit (Additional file 1: Fig. S1A and S1B). The P8 constitutive promoter was employed to express the AHL synthase EsaI in the inhibition unit as previously described [25]. For circuit characterization, sfGFP was used as the reporter in the response unit. The basal state was measured from the strain harboring only the response unit, the activation state was measured from the strain harboring the activation unit and the response unit, and the activation & inhibition state was measured from the strain harboring the activation unit, the inhibition unit, and the response unit [30]. Continuous fluorescence measurements were performed, and the fluorescence was normalized by OD_{600} . The activation fold was defined as the ratio of normalized peak fluorescence in the activation state to that in the basal state, and the inhibition fold was defined as the ratio of normalized peak fluorescence in the activation state to that of the activation & inhibition state.

We first characterized the performance of the Esa- P_{esaS} circuit in M9 medium at neutral pH (7.0) as shown in Fig. S1C. The basal state showed a relatively low level of normalized fluorescence, comparable to the autofluorescence measured from the cells alone. The activation state exhibited constitutively increasing normalized fluorescence, as anticipated. The activation & inhibition state displayed a desired pulse-like pattern of normalized fluorescence, rising from the outset, peaking around 6 h, and subsequently declining and stabilizing at approximately 12 h (Additional file 1: Fig. S1C). These results demonstrated that the dual-plasmid based Esa- P_{esaS} circuit operated effectively in the *E. coli* DH10B strain under neutral pH condition, achieving an activation fold of 52.2 and an inhibition fold of 15.5.

We then characterized the Esa- P_{esaS} circuit in the *E. coli* MG1655 in LBG medium under three different pH conditions (i.e. pH 7.0, 5.5, and 4.5), commonly employed for acid resistance evaluation [19, 20]. We used mCherry as reporter due to its lower background fluorescence and higher stability in acidic LBG mediums than sfGFP [39]. As shown in Fig. 1B, under each pH condition, the basal state exhibited the lowest normalized peak fluorescence, followed by the activation & inhibition state, with the activation state showing the highest normalized peak

fluorescence. The activation folds were 16.4, 4.2, and 1.9, and inhibition folds were 5.8, 1.5, and 1.4, respectively, at pH 7.0, 5.5, and 4.5 (Fig. 1C). These activation folds and inhibition folds displayed a significant decrease as the pH decreased, even dropping below 2 at pH 4.5, indicating a loss of function of the Esa- P_{esaS} circuit. Ideally, the activation folds should surpass 10, and the inhibition folds should exceed 2 [40–42].

We observed that the normalized peak fluorescence in the activation state remained relatively stable across all three pH conditions. However, the normalized peak fluorescence in the basal state and the activation & inhibition state exhibited significant increases in the pH response ratios (defined as the ratio of normalized peak fluorescence in each state at pH 4.5 to that at pH 7.0) of 11.1-fold and 5.2-fold, respectively (Fig. 1B). These findings

indicated that the P_{esaS} promoter was somehow activated under low pH conditions in the absence or presence of EsaRI70V.

Decoupling of the quorum sensing function of P_{esaS} promoter from low-pH crosstalk

Therefore, we analyzed and engineered the P_{esaS} promoter to decouple the quorum sensing function from the low-pH crosstalk. Figure 2A illustrates the division of the 184 base pairs-long P_{esaS} promoter into four segments [25, 30, 43]: segment A, the upstream sequence (-184 to -87, 98 bp); segment B, the essential *esa* box (-86 to -67, 20 bp); segment C, the spacer (-66 to -46, 21 bp) that locates between segments B and D.

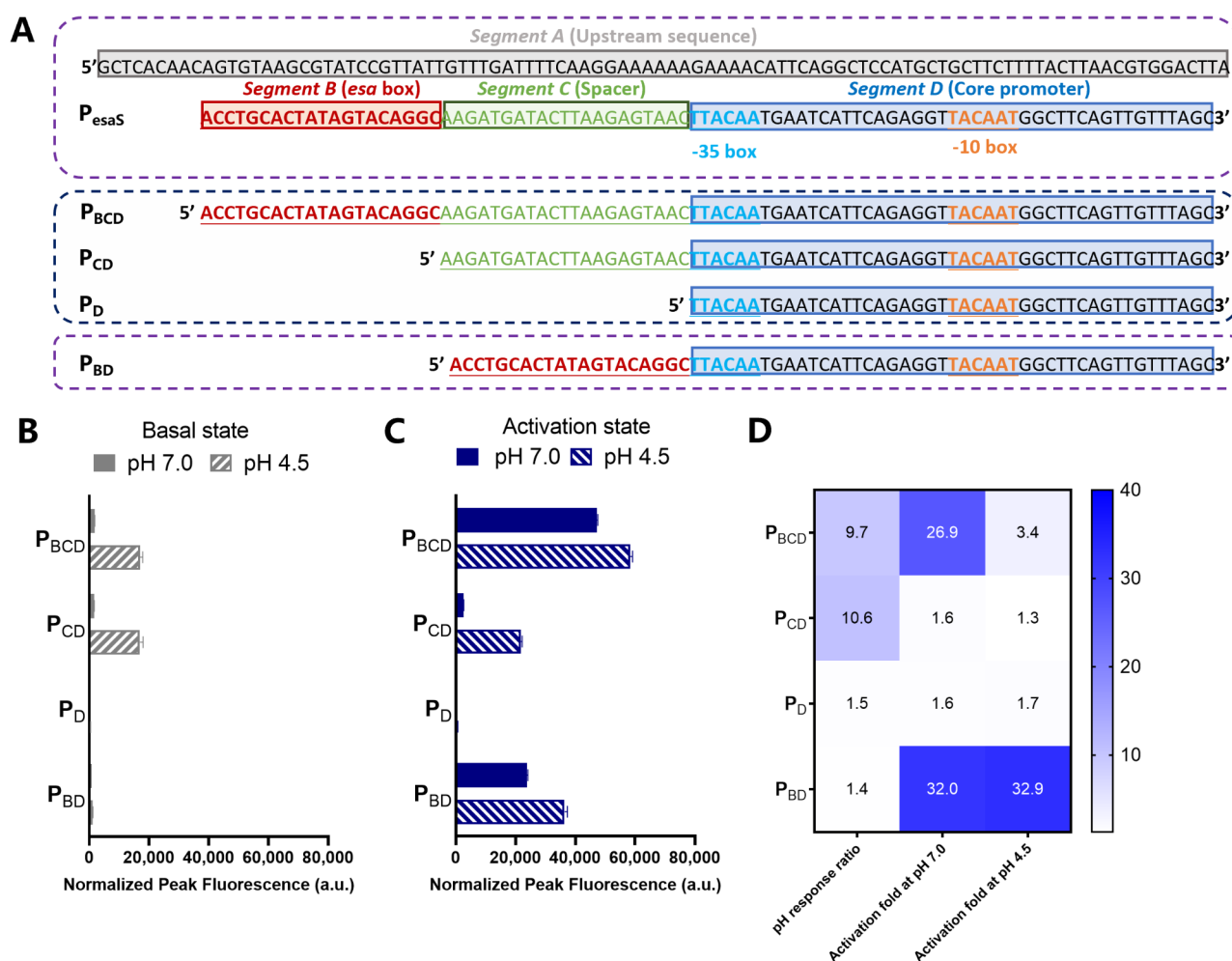


Fig. 2 Construction and characterization of P_{esaS} variants. **(A)** Schematic diagram of P_{esaS} and the variants. The P_{esaS} promoter was divided into 4 segments A, B, C, and D. Segment A is the upstream sequence of the *esa* box, segment B is *esa* box, segment C is the native spacer, and segment D is the core promoter of P_{esaS} . **(B)** The normalized peak fluorescence in basal states of circuits using P_{esaS} or the variants as response promoter in LBG medium at pH 7.0 and pH 4.5. **(C)** The normalized peak fluorescence in activation states of circuits using P_{esaS} or the variants as response promoter in LBG medium at pH 7.0 and pH 4.5. **(D)** The pH response ratios of P_{esaS} and the variants, and activation folds of circuits that utilized them as response promoter at pH 7.0 and pH 4.5. Data are presented as mean \pm s.d. of three replicates

We first constructed three truncated promoters, P_{BCD} , P_{CD} , and P_D , by progressively deleting segments A, B, and C, and evaluating the pH response ratios and activation folds in LBG medium at pH 7.0 and 4.5 (Fig. 2B and D). As shown in Fig. 2D, only the P_D promoter exhibited a significantly lower pH response ratio of 1.5-fold, indicating that segment C likely contributes to the low-pH crosstalk of the P_{esaS} promoter. Besides, the P_{BCD} exhibited a pH response ratio of 9.7-fold, comparable to that of the P_{esaS} (11.1-fold), and an activation fold of 26.9 at pH 7.0, even slightly surpassing that of the P_{esaS} (16.4), suggesting that segment A does not seem to influence the pH response or the quorum sensing function. Consequently, we reconstituted a new promoter, P_{BD} , by directly placing the *esa* box upstream of the core promoter. Figure 2D demonstrated that the P_{BD} promoter yielded a pH response ratio of 1.4-fold, and activation folds of 32.0 and 32.9 at pH 7.0 and 4.5, respectively. Additionally, at pH 5.5, the P_{BD} promoter showed an activation fold of 26.3 (Additional file 1: Fig. S2B). These results elucidated that segment B (the *esa* box) does not contribute to low pH crosstalk, and that the P_{BD} promoter restores the quorum sensing function under acidic conditions. Further analysis via the Position weight matrix (PWM) of the P_{esaS} promoter sequence by Virtual Footprint [44] revealed potential low-pH activation by YhiX (renamed GadX, Additional file 2: Table S1), known to respond to low pH and CRP [45, 46]. Our preliminary results showed that this spacer could indeed enhance promoter strength at pH 4.5 without altering strength at pH 7.0 (Additional file 1: Fig. S3).

To assess circuit robustness, we supplementally measured the activation folds and inhibition folds for both the $Esa-P_{esaS}$ and the $Esa-P_{BD}$ circuits in MG1655 in LB and M9 mediums at pH 7.0, 5.5 and 4.5, and calculated coefficient of variation (CV, the ratio of the standard deviation to the mean) under the nine culture conditions [47] (Additional file 1: Fig. S2). The $Esa-P_{BD}$ circuit exhibited higher conservation than the $Esa-P_{esaS}$ circuit in both activation folds (CV of 0.16 vs. 0.62) and inhibition folds (CV of 0.06 vs. 0.50) cross these culture conditions, indicating that the $Esa-P_{BD}$ circuit is more robust than the $Esa-P_{esaS}$ circuit.

Fine tuning of the $Esa-P_{BD}$ circuit

In 96-well plate experiments, we noticed that the MG1655 strain harboring the activation and response units showed a reduced growth rate, although the strain containing the activation, inhibition, and response units (or the complete $Esa-P_{BD}$ circuit) remained unaffected. In addition, when the $Esa-P_{BD}$ AR circuit was introduced into an industrial lysine-producing strain *E. coli* SCEcL3, the engineered strain exhibited a significantly lower growth rate in a preliminary 5-L fermentation test (data

not shown). We then replaced the backbone pACYC184 (p15A ori, 15 copies) for the regulator plasmid with the lower-copy backbone pZS1 (pSC101 ori, 4 copies), yielding the $Esa-P_{BD}(L)$ circuit [37], which restored the normal growth rate both for MG1655 in the 96-well format (Additional file 1: Fig. S4A), and for the industrial SCEcL3 strain in a 5-L fermentation test (Additional file 1: Fig. S6).

To introduce greater diversity into the $Esa-P_{BD}(L)$ circuit, we employed three additional growth phase-related promoters (P38, P84, and P374) for the expression of *EsaI*. These promoters exhibit similar strength but theoretically differ in the induction times relative to the entry time for the stationary phase (-1.5 h, +0.5 h, and +0.75 h, respectively) [25, 48]. The $Esa-P_{BD}(L)$ circuits employing P8, P38, P84, and P374 exhibited inhibition folds of 4.4, 2.7, 4.8, and 2.0 (Additional file 1: Fig. S4B), respectively, in LBG medium at pH 7.0.

Incorporation of AR module into the $Esa-P_{BD}(L)$ circuits

As previously stated, the AR module used in our study consists of Hfq and DsrA. To simplify the co-expression, we placed them under a single P_{BD} promoter, and inserted a classic hammerhead ribozyme [49] (Additional file 1: Fig. S5A). The Hammerhead (HH) ribozyme self-cleaves at the 3'-end of its mRNA to release the sRNA DsrA, with a cleavage efficiency of approximately 74% as demonstrated by real-time quantitative PCR [50] (Additional file 2: Table S2).

Subsequently, these $Esa-P_{BD}(L)$ AR circuits were introduced into the MG1655 strain, yielding four MG/AR(XX) strains (XX represents the different promoters used for the expression of *EsaI*, i.e., XX=P8, P38, P84, P374, Additional file 2: Table S3). The growth performance of these engineered strains was evaluated in LBG medium at pH 5.5 and 4.5. As shown in Fig. S5B, all four strains showed improved growth compared to the MG1655 strain, with final OD_{600} values increased by 19–36% at pH 4.5, and 14–44% at pH 5.5, respectively. Additionally, MG/AR(P8) and MG/AR(P374) demonstrated higher maximum growth rates (μ_{max}), enhanced by 9.7% and 9.4% at pH 4.5, and 9.5% and 10.9% at pH 5.5, respectively. We also evaluated strain containing the AR module in activation state (MG/AR(AS) strain). While the final OD_{600} of MG/AR(AS) increased by 15.2% at pH 4.5 and 37.9% at pH 5.5 compared to MG1655, the μ_{max} decreased by 16.8% at pH 4.5 and 12.2% at pH 5.5, suggesting potentially detrimental effects on cell growth with AR module keeping expressing. These results indicated that $Esa-P_{BD}(L)$ AR circuits effectively conferred acidic resistance to the laboratory model strain *E. coli* MG1655 under moderate acid stress.

Application of the $Esa-P_{BD}(L)$ AR circuits for enhancing productivity of an industrial *E. coli* strain at pH 5.5

To evaluate the potential of $Esa-P_{BD}(L)$ AR circuits in enhancing the productivity of the industrial *E. coli* strain under acidic condition in a scaled-up process, we introduced the $Esa-P_{BD}(L)$ AR circuits into the industrial lysine-producing strain *E. coli* SCEcL3, yielding four SC/AR(XX) strains (XX=P8, P38, P84, P374, Additional file 2: Table S3). Fermentation was conducted in fed-batch mode in 5-L parallel bioreactors using an industrial-grade lysine fermentation medium (LFM) provided by China Oil & Foodstuffs Corporation (COFCO).

As the control, the parent strain SCEcL3 was cultured at pH 6.8 and 5.5 for 48 h in fed-batch mode, with the initial pH of the medium set at 6.8 (Fig. 3, and Additional file 1: Fig. S6). SCEcL3 achieved a lysine titer of 103 g/L, a yield of 0.51 g/g, a productivity of 2.15 g/(L·h), an ammonia consumption of 505 mL, and a final OD_{562} of 30, at pH 6.8. And these values were 92 g/L, 0.47 g/g, 1.92 g/(L·h), 397 mL, and 37 at pH 5.5, respectively, corresponding to 89%, 92%, 89%, 79%, and 123% respectively, of those observed for SCEcL3 at pH 6.8. Subsequently, the four engineered SC/AR(XX) strains (XX=P8, P38, P84, P374) were fermented in fed-batch mode at pH 5.5. As shown in Fig. 3, SC/AR(P8) achieved a lysine titer of 102 g/L, a yield of 0.53 g/g, a productivity of 2.13 g/(L·h), an ammonia consumption of 398 mL, and a final OD_{562} of 30 at pH 5.5. These values corresponded to 99%, 104%, 99%, 79%, and 100% respectively, of those observed for SCEcL3 at pH 6.8, or 111%, 113%, 111%, 100%, and 81% respectively, of those observed for SCEcL3 at pH 5.5. Similar, albeit less pronounced, trends were observed for SC/AR(P38) and SC/AR(P84). However, SC/AR(P374) did not show enhanced fermentation performance at pH 5.5 compared to SCEcL3. Fed-batch fermentations of SCEcL3 and three engineered strains SC/AR(P8), SC/AR(P38), and SC/AR(P84) at pH 5.0 were also conducted. Though performance of three engineered strains were superior to that of SCEcL3, all were inferior to that of SCEcL3 at pH 6.8 (data not shown). These results demonstrated that the AR module, under the robust gene expression control of the $Esa-P_{BD}(L)$ circuits, effectively enhances acid tolerance and preserves the productivity robustness for the industrial lysine-producing strain *E. coli* SCEcL3 under acidic stress.

Discussion

Improving acid resistance and productivity robustness of strains under moderate acid conditions presents an enduring challenge in industrial bioprocesses [12, 19, 51]. In this study, we successfully constructed the $Esa-P_{BD}(L)$ AR circuits, which conferred an *E. coli* industrial strain with comparable fermentation performance at pH 5.5 to that of the parent strain at pH 6.8 in fed-batch mode.

Rough estimates suggest that fermenting at pH 5.5 led to approximately a 4% reduction in glucose consumption and a 10% reduction in ammonia consumption, along with a 16% reduction in acid usage needed for extraction [52] (Fig. 3). To our knowledge, this is the lowest pH condition reported so far tolerable for a lysine-producing industrial *E. coli* strain in 5-L bioreactors, while maintaining productivity. This work serves as an example of how to employ gene circuits in scaled-up bioprocesses to enhance the stress tolerance and productivity robustness of industrial strains.

As mentioned in the background section, *E. coli* is more sensitive to acid stress in the exponential phase, but becomes more acid-tolerant in the stationary phase [16–18]. In this study, we engineered an “ON to OFF” genetic circuit that enhances the expression of AR-related genes during the exponential phase while suppressing this enhanced expression during the stationary phase. Our results from 5-L fed-batch fermentation validated this design.

The applications of genetic circuits in industrial environments remain challenging due to their inherently greater complexity compared to well-controlled laboratory conditions [34]. These circuits are typically constructed using regulatory parts derived from natural organisms, such as the P_{esaS} promoter utilized in our study, which are often influenced by multiple biotic and abiotic factors [53–57]. Consequently, these circuits may exhibit markedly different behavior outside of laboratory settings. Our work provides an illustration of how a genetic circuit can become dysfunctional under acidic conditions, as the P_{esaS} promoter contained an unknown element responsive to acidity. However, our success in devising the $Esa-P_{BD}(L)$ AR circuits suggests that the complexity issues can be addressed through further synthetic design. This involves decoupling co-regulation and insulating circuit function from more complex environmental conditions. Lastly, this study reaffirms the utility of a stepwise evaluation scheme for assessing stress tolerance modules or circuits [14]. This includes (1) initially screening their functions in laboratory model strains in microplates to enhance throughput, and (2) selectively evaluating their functions in the intended industrial strains in bioreactors.

Conclusion

This study demonstrates an effective strategy to enhance the acid tolerance and productivity of an industrial *E. coli* strain in scaled-up bioprocesses employing quorum sensing-based gene circuits. By engineering the P_{esaS} promoter to restore quorum sensing function, and incorporating the AR module into the $Esa-P_{BD}(L)$ circuit, we achieved robust lysine production at pH 5.5. The $Esa-P_{BD}(L)$ AR circuits were fine-tuned and validated through

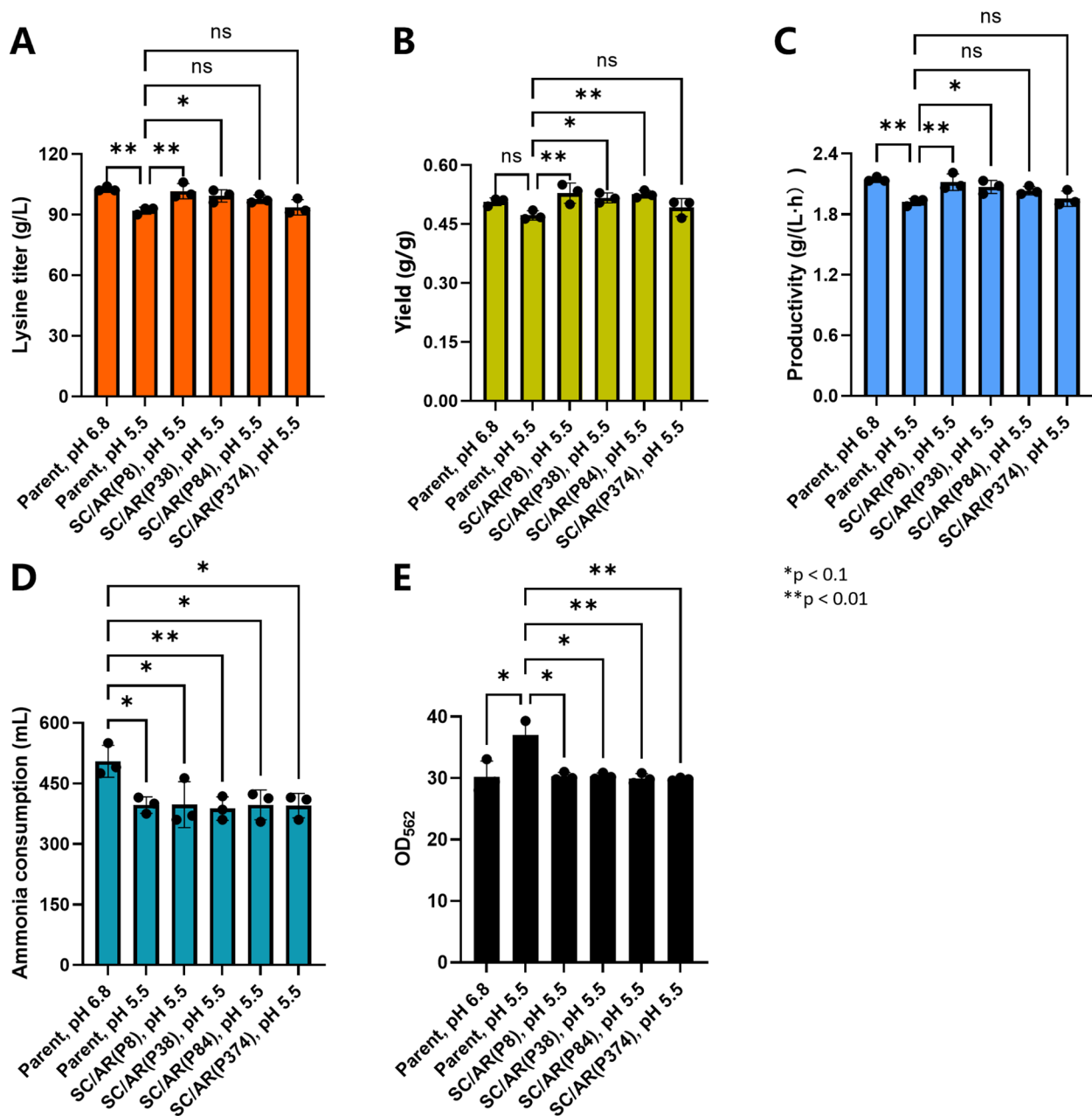


Fig. 3 Application of Esa-P_{BD}(L) AR circuits in industrial strain SCEcL3 in 5-L bioreactor. lysine titer (**A**), yield (**B**), productivity (**C**), ammonia consumption (**D**), and OD₅₆₂ (**E**) of the industrial lysine-producing strain *E. coli* SCEcL3 harboring different Esa-P_{BD}(L) AR circuits and the parent strain SCEcL3 fermented in fed-batch mode in 5-L bioreactor in an industrial grade fermentation medium for 48 h. Fermentation performance of the parent strain SCEcL3 was evaluated at pH 6.8 and pH 5.5, respectively. Fermentation performances of four engineered strains SC/AR(P8), SC/AR(P38), SC/AR(P84), and SC/AR(P374) were evaluated at pH 5.5

* Represents significance ($p < 0.1$), and ** represents significance ($p < 0.01$). Data are presented as mean \pm s.d. of three replicates

a stepwise evaluation, starting with high-throughput screenings in laboratory strain and progressing to fermentation performance evaluations in industrial strain. This approach highlights the potential of synthetic biology to address stress-related challenges in industrial bioprocessing, offering a scalable solution to improve process efficiency and sustainability.

Methods and materials

Strains, plasmids, and materials

The strains and plasmids used in this study are summarized in Additional file 2: Table S3. The DNA sequences of primers used in this study are listed in Additional file 2: Table S4, and sequences for linear DNA templates used in this study are listed in Additional file 2: Table

S5. Q5 DNA polymerase and Gibson Assembly Master Mix were purchased from New England Biolabs (Beverly, MA, USA). pCOLA-T7-WspR and pZS1-ITlrLLtCL were purchased from Addgene (Watertown, MA, USA) for cloning the pCOLADuet-1 and the pZS1 backbone. Oligonucleotides synthesis and sequence analysis were performed by Sangon Biotech (Shanghai, China) and RuiBiotech (Beijing, China). The kits for DNA purification, gel recovery, and plasmid mini-prep were purchased from Tiangen (Beijing, China) and Magen (Guangzhou, China). The 96 well black flat clear bottom polystyrene microplates were purchased from Corning (New York, USA). The 100 well Honeycomb microplates were purchased from OY (Oy Growth Curves Ab Ltd., Helsinki, Finland). All chemicals were purchased from Sigma-Aldrich (Shanghai, China) or Sangon Biotech (Shanghai, China).

Culture media

For cloning, all *E. coli* DH10B and *E. coli* MG1655 strains were cultured in Luria-Bertani (LB) medium at 37 °C [19]. For the circuit characterization, all *E. coli* DH10B strains were tested in M9 medium, and all *E. coli* MG1655 strains were tested in LB medium supplemented with 20 g/L glucose (LBG medium), which was also acidified by HCl to pH 5.5 or pH 4.5. For the cell growth assay, all *E. coli* MG1655 strains were tested in LBG medium at three pH conditions, too. For fermentation of *E. coli* MG1655 SCEcL3 strains, the seed medium consisted of sucrose (3 g/L), yeast extract (5 g/L), tryptone (7 g/L), ammonium sulfate (5 g/L), potassium dihydrogen phosphate (5 g/L), magnesium sulfate (0.5 g/L), ferrous sulfate (0.012 g/L), manganous sulfate (0.012 g/L), sodium glutamate (5 g/L), l-threonine (0.3 g/L), l-methionine (0.3 g/L) and pyruvic acid (0.3 g/L), and the fermentation medium consisted of glucose (30 g/L), phosphoric acid (0.6 g/L), magnesium sulfate (2 g/L), ammonium sulfate (10 g/L), corn steep liquor (6.5 g/L), hydrolyzed feather meal (6.5 g/L), potassium chloride (0.5 g/L), betaine (2.2 g/L), ferrous sulfate (0.032 g/L), manganous sulfate (0.032 g/L), l-threonine (0.25 g/L), cupric sulfate (6.8 mg/L), zinc sulfate (7.65 mg/L), and thiamine (5.6 mg/L). For the strains harboring plasmids with chloramphenicol, kanamycin or carbenicillin resistance, 34 µg/mL chloramphenicol, 50 µg/mL kanamycin, or 100 µg/mL carbenicillin was added to the medium.

Gene circuit construction

The dual-plasmid system used in this study contained the regulator and response plasmids. For the regulator plasmid, the medium-copy plasmid pACYC184 (~15 copies per cell) or the low-copy plasmid pZS1 (~4 copies per cell) was used as the backbone [37]. To fine tune the expression level of *EsaRI70V*, *esaRI70V* was placed

under a series of PJ231XX promoters [38] with the constant Bujard RBS [58]. To fine tune the expression level of *EsaI*, *esaI* was placed under a constant P8 promoter [59] or the growth related P38, P84, and P374 promoter [48] with a constant BCD22 RBS [59]. For the response plasmid, the low-copy plasmid pCOLADuet-1 (~5 copies per cell) was used as the backbone [25, 37]. The P_{esaS} promoter or P_{esaS} -derived variants with the constant Bujard RBS were placed upstream of the reporter gene, *sfGFP* or *mCherry* to construct response plasmids. Specifically, for decoupling the quorum sensing function of the P_{esaS} promoter from the low-pH crosstalk, some variants were designed and constructed by corresponding primers, and then incorporated into the corresponding backbones. All plasmids were constructed using the Gibson assembly method [60].

Gene circuit characterization

For characterizing *Esa* QS circuits, *in vivo* OD and fluorescence measurement were conducted by plate reader experiment. Engineered strains were firstly inoculated in 2 mL LB medium with corresponding antibiotics and grown overnight at 37 °C with 220 rpm. The overnight cultures were diluted to OD₆₀₀ of 0.01 with tested medium, and then 4 µL diluted cultures were added into 196 µL tested medium in 96-well black flat clear bottom polystyrene microplates [61]. The cultures were grown at 37 °C for 24 h, and OD₆₀₀ and fluorescence were determined by Tecan infinite 200 pro microplate reader (Tecan Group Ltd., Männedorf, Switzerland). The emission and excitation wavelengths were 514 nm, 385 nm for *sfGFP*, and 635 nm, 588 nm for *mCherry*. For plate reader experiments, each experiment was performed in triplicate through inoculating into different wells in 96-well microplates and the averaged values were used for analysis. Each experiment was performed in three biological replicates.

Robustness analysis

The activation folds and inhibition folds of the *Esa*- P_{esaS} and *Esa*- P_{BD} circuits in nine culture conditions (LBG, LB, and M9 mediums with pH 7.0, 5.5, and 4.5 each) were used to calculate CV values by GraphPad Prism 9.0.0.

Hammerhead Ribozyme cleavage efficiency analysis

The MG/AR(P8) strain was cultured in LBG medium, and sampled at exponential phase (EP) and stationary phase (SP), respectively. The total RNAs were extracted from 2 OD units of cells by using the TRIzol reagent kit (Invitrogen, CA, USA), and the cDNAs were obtained by using the PrimeScript RT reagent kit gDNA Eraser (TaKaRa, Dalian, China) according to the manufacturer's instructions as previous described [19]. Primer locations were indicated in Additional file 1: Fig. S5A, and

DNA sequences of primers were listed in Additional file 2: Table S4. The RT-qPCR assays were performed using the CFX Connect Real-Time PCR Detection System (Bio-Rad). Three technical replicates of each gene and three biological replicates of each strain were analyzed to allow for statistical analysis. The relative amounts of Hfq and HD (the Hfq-HH-DsrA module) were normalized by the 16s RNA of each sample, and the ratio of Hfq to HD was determined using the comparative threshold cycle number ($2^{-\Delta\Delta CT}$) method,

$$Ratio_{(Hfq/HD)} = 2^{-((CT_{Hfq}-CT_{16s})-(CT_{HD}-CT_{16s}))}$$

and cleavage efficiency was calculated as following formula described previously [50]:

$$Cleavage\ efficiency = 100\% - 100\% * \frac{1}{Ratio_{(Hfq/HD)}}$$

Acid resistance engineered strains construction and cell growth assay

For constructing $Esa-P_{BD}(L)$ -based acid resistance gene circuits, we placed the AR module under the P_{BD} promoter and the Bujard RBS. In the AR module, we inserted the HH ribozyme between genes of *hfq* and *dsrA*, and the *dsrA* gene contains its native terminator. Specifically, the design of the HH ribozyme followed the previously described method [49, 62]. Then $Esa-P_{BD}(L)$ AR circuits were introduced into MG1655 strain. The cell growth assay was performed using a modification of the protocol as described in our pervious study [12, 14, 19]. *E. coli* MG1655 and strains harboring $Esa-P_{BD}(L)$ AR circuit were cultured overnight in LBG medium (pH 7.0) at 37 °C, and then the cultures were diluted to initial OD_{600} of 0.05 in 300 μ L LBG medium at pH 5.5 and pH 4.5. Then the cultures were incubated at 37 °C in 100-well Honeycomb microplates and OD_{600} was determined by automated turbidimeter (Bioscreen C, Oy Growth Curves Ab Ltd., Helsinki, Finland) for 24 h. Each experiment was performed in three biological replicates.

Lysine fermentation in 5-L bioreactors

Fermentation test was performed in 5-L parallel-bioreactors (T&J Bio-engineering Co. LTD, Shanghai). Engineered strains harboring $Esa-P_{BD}(L)$ AR circuit were inoculated in 10 mL seed medium and cultured for 14 h at 37 °C with 220 rpm. Then 6 mL seed inoculums were inoculated into 300 mL fresh seed medium and grown overnight at 37 °C with 220 rpm for enlarged culture. Then 300 mL seed inoculums were inoculated into 1700 mL fermentation medium in bioreactors. The temperature, pH and DO were monitored online during the 48 h fermentation period. The DO, pH and temperature were

monitored online. The pH of culture was set at 6.8 at the beginning, and controlled at 6.8 or 5.5 by the addition of 12.5% (w/v) ammonia during the fermentation. DO, temperature, and glucose were controlled at 40–60%, 37.0 ± 0.1 °C, and 0.4–0.8% (w/v), respectively, during the 48 h fermentation period. DO was monitored online and was controlled by adjusting the agitation rate from 200 to 1000 rpm with an aeration rate of 0.5 vvm. Samples were taken periodically for measuring optical density, residual glucose, and lysine. The optical density was measured at 562 nm (OD_{562}) [63] by ultraviolet spectrophotometer (UV755B, Yoke Instrument, Shanghai, China), and residual glucose, and lysine were measured by using SBA-40D biosensor analyzer (Shandong Academy of Science, Shandong Province, China). Each experiment was performed in three biological replicates.

Abbreviations

<i>E. coli</i>	<i>Escherichia coli</i>
AR	Acid resistance
QS	Quorum sensing
AHL	N-Acyl homoserine lactone
DO	Dissolved oxygen
OD_{600}	Optical density at 600 nm
OD_{562}	Optical density at 562 nm
RT-qPCR	Real-time quantitative PCR
PWM	Position weight matrix
sRNA	Small RNA

Supplementary Information

The online version contains supplementary material available at <https://doi.org/10.1186/s12934-024-02524-9>.

Additional file 1: Figure S1: Optimization of the expression level of *Esa-P_{BD}*. **Figure S2:** Characterization of *Esa-P_{esAs}* and *Esa-P_{BD}* circuits. **Figure S3:** Characterization of the engineered acid-response promoters. **Figure S4:** Fine tuning of the *Esa-P_{BD}* circuit. **Figure S5:** Design and evaluation of the *Esa-P_{BD}*(L)-based AR circuits. **Figure S6:** Lysine titer, OD_{562} and glucose of strains during fermentation in 5-L bioreactors

Additional file 2: Table S1: Position weight matrix analysis of the P_{esAs} by Virtual Footprint. **Table S2:** CT values of Hfq and HD of each sample and cleavage efficiency that determined by RT-qPCR. **Table S3:** Strains and plasmids used in this study. **Table S4:** DNA sequences of primers used in this study. **Table S5:** DNA sequences of genes used in this study

Author contributions

ZL, XYang, and XYan conceived the ideas and designed the framework. XYan and AB performed most of the experiments. YY and XZ assisted in the fermentation experiments. ZL, XYang, and XYan analyzed the data, and all authors discussed the results. XYang and XYan prepared the initial draft of the manuscript. ZL and XYang revised the manuscript.

Funding

This study was supported by the National Key R&D Program of China (2018YFA0901000), and the Guangdong Basic and Applied Basic Research Foundation (2024A1515030121).

Data availability

No datasets were generated or analysed during the current study.

Declarations

Ethics approval and consent to participate

Not applicable.

Consent for publication

Not applicable.

Competing interests

Xiaofeng Yang, Zhanglin Lin, Xiaofang Yan, and Anqi Bu are filing two patents (CN202211426889.0, CN202211457606.9) on aspects of this work.

Received: 18 June 2024 / Accepted: 6 September 2024

Published online: 28 September 2024

References

- OECD. The Bioeconomy to 2030/2009.
- Lin Z, Zhang YP, Wang J. Engineering of transcriptional regulators enhances microbial stress tolerance. *Biotechnol Adv.* 2013;31(6):986–91.
- Cortés J, Flores N, Bolívar F, Lara AR, Ramírez OT. Physiological effects of pH gradients on *Escherichia coli* during plasmid DNA production. *Biotechnol Bioeng.* 2016;113:598–611.
- Rutherford BJ, Dahl RH, Price RE, Szmidt HL, Benke PI, Mukhopadhyay A, et al. Functional genomic study of exogenous n-Butanol stress in *Escherichia coli*. *Appl Environ Microbiol.* 2010;76:1935–45.
- Zaldivar J, Ingram LON. Effect of organic acids on the growth and fermentation of ethanologenic *Escherichia coli* LY01. *Biotechnol Bioeng.* 1999;66:4.
- Russell JB, Diez-Gonzalez F. The effects of fermentation acids on bacterial growth. *Adv Microb Physiol.* 1998;39:205–34.
- Warnecke T, Gill RT. Organic acid toxicity, tolerance, and production in *Escherichia coli* biorefining applications. *Microb Cell Fact.* 2005;4:25.
- Ma H, Kumar B, Ditzes U, Gunzer F, Buer J, Zeng A-P. An extended transcriptional regulatory network of *Escherichia coli* and analysis of its hierarchical structure and network motifs. *Nucleic Acids Res.* 2004;32(22):6643–9.
- Kanjee U, Houry WA. Mechanisms of acid resistance in *Escherichia coli*. *Annu Rev Microbiol.* 2013;67:65–81.
- Alper HS, Stephanopoulos G. Global transcription machinery engineering: a new approach for improving cellular phenotype. *Metab Eng.* 2007;9(3):258–67.
- Chen T, Wang J, Yang R, Li J, Lin M, Lin Z. Laboratory-evolved mutants of an Exogenous Global Regulator, IrrE from *Deinococcus radiodurans*, enhance stress tolerances of *Escherichia coli*. *PLoS ONE.* 2011;6:e16228.
- Gao X, Yang X, Li J, Zhang YP, Chen P, Lin Z. Engineered global regulator H-NS improves the acid tolerance of *E. Coli*. *Microb Cell Fact.* 2018;17:118.
- Basak S, Geng H, Jiang R. Rewiring global regulator cAMP receptor protein (CRP) to improve *E. Coli* tolerance towards low pH. *J Biotechnol.* 2014;173:68–75.
- Yao X, Liu P, Chen B, Wang X, Tao F, Lin Z, et al. Synthetic acid stress-tolerance modules improve growth robustness and lysine productivity of industrial *Escherichia coli* in fermentation at low pH. *Microb Cell Fact.* 2022;21(1):68.
- Kim HJ, Turner TL, Jin YS. Combinatorial genetic perturbation to refine metabolic circuits for producing biofuels and biochemicals. *Biotechnol Adv.* 2013;31(6):976–85.
- Richard H, Foster JW. *Escherichia coli* Glutamate- and arginine-dependent Acid Resistance systems increase Internal pH and reverse transmembrane potential. *J Bacteriol.* 2004;186:6032–41.
- Xu Y, Zhao Z, Tong W, Ding Y, Liu B, Shi Y, et al. An acid-tolerance response system protecting exponentially growing *Escherichia coli*. *Nat Commun.* 2020;11(1):1496.
- Richard HT, Foster JW. Acid resistance in *Escherichia coli*. *Adv Appl Microbiol.* 2003;52:167–86.
- Lin Z, Li J, Yan X, Yang J, Li X, Chen P, et al. Engineering of the small noncoding RNA (sRNA) DsrA together with the sRNA chaperone hfq enhances the Acid Tolerance of *Escherichia coli*. *Appl Environ Microbiol.* 2021;87(10):e02923–20.
- Gaida SM, Al-Hinai MA, Indurthi DC, Nicolaou SA, Papoutsakis ET. Synthetic tolerance: three noncoding small RNAs, DsrA, ArcZ and RprA, acting supra-additively against acid stress. *Nucleic Acids Res.* 2013;41:8726–37.
- Battesti A, Majdalani N, Gottesman S. The RpoS-mediated general stress response in *Escherichia coli*. *Annu Rev Microbiol.* 2011;65:189–213.
- Zhou Y, Gottesman S. Modes of regulation of RpoS by H-NS. *J Bacteriol.* 2006;188:7022–5.
- Battesti A, Tsegaye YM, Packer DG, Majdalani N, Gottesman S. H-NS regulation of IraD and IraM antiadaptors for control of RpoS degradation. *J Bacteriol.* 2012;194:2470–8.
- Zhang W, Zhu J, Zhu X, Song M, Zhang T, Xin F, et al. Expression of global regulator IrrE for improved succinate production under high salt stress by *Escherichia coli*. *Bioresour Technol.* 2018;254:151–6.
- Gupta A, Reizman I, Reisch CR, Prather K. Dynamic regulation of metabolic flux in engineered bacteria using a pathway-independent quorum-sensing circuit. *Nat Biotechnol.* 2017;35:273–9.
- Ge C, Yu Z, Sheng H, Shen X, Sun X, Zhang Y, et al. Redesigning regulatory components of quorum-sensing system for diverse metabolic control. *Nat Commun.* 2022;13(1):2182.
- Holtz WJ, Keasling JD. Engineering Static and Dynamic Control of Synthetic pathways. *Cell.* 2010;140:19–23.
- Zhou L, Zeng A. Exploring lysine riboswitch for metabolic flux control and improvement of L-lysine synthesis in *Corynebacterium glutamicum*. *ACS Synth Biol.* 2015;4:6729–34.
- Sun Z, Wei W, Zhang M, Shi W, Zong Y, Chen Y, et al. Synthetic robust perfect adaptation achieved by negative feedback coupling with linear weak positive feedback. *Nucleic Acids Res.* 2022;50:2377–86.
- Schu DJ, Carlier A, Jamison KP, von Bodman SB, Stevens AM. Structure/Function analysis of the *Pantoea stewartii* Quorum-Sensing Regulator EsaR as an activator of transcription. *J Bacteriol.* 2009;191:7402–9.
- Liu C, Fu X, Liu L, Ren X, Chau CK-I, Li S, et al. Sequential establishment of stripe patterns in an Expanding Cell Population. *Science.* 2011;334:238–41.
- Ma Y, Budde MW, Mayalu MN, Zhu J, Lu AC, Murray RM, et al. Synthetic mammalian signaling circuits for robust cell population control. *Cell.* 2020;185:967–79.
- Bradley B RW, Buck, M, Wang. Tools and principles for Microbial Gene Circuit Engineering. *J Mol Biol.* 2016;428(5 Pt B):862–88.
- Lezia A, Miano A, Hasty J. Synthetic gene circuits: design, implement, and apply. *Proc IEEE.* 2022;110:613–30.
- Wu J, Bao M, Duan X, Zhou P, Chen C, Gao J, et al. Developing a pathway-independent and full-autonomous global resource allocation strategy to dynamically switching phenotypic states. *Nat Commun.* 2020;11:5521.
- Shong J, Huang Y-m, Bystroff C, Collins CH. Directed evolution of the quorum-sensing regulator EsaR for increased signal sensitivity. *ACS Chem Biol.* 2013;8:4789–95.
- Shao B, Rammohan J, Anderson DA, Alperovich N, Ross D, Voigt CA. Single-cell measurement of plasmid copy number and promoter activity. *Nat Commun.* 2021;12:1475.
- Anderson JC. Anderson promoter collection. 2015. <http://parts.igem.org/Promoters,Catalog/Anderson>
- Botman D, de Groot DH, Schmidt P, Goedhart J, Teusink B. In vivo characterization of fluorescent proteins in budding yeast. *Sci Rep.* 2018;9:2234.
- Litovco P, Barger N, Li X, Daniel R. Topologies of synthetic gene circuit for optimal Fold change activation. *Nucleic Acids Res.* 2021;49:5393–406.
- Zeng W, Du P, Lou Q, Wu L, Zhang H, Lou C, et al. Rational design of an ultra-sensitive quorum-sensing switch. *ACS Synth Biol.* 2017;6(8):1445–52.
- Brophy JAN, Voigt CA. Principles of genetic circuit design. *Nat Methods.* 2014;11:508–20.
- von Beck S, Farrand SK. Capsular polysaccharide biosynthesis and pathogenicity in *Erwinia stewartii* require induction by an N-acylhomoserine lactone autoinducer. *J Bacteriol.* 1995;177:5000–8.
- Münch R, Hiller K, Grote A, Scheer M, Klein J, Schobert M, et al. Virtual footprint and PRODORIC: an integrative framework for regulon prediction in prokaryotes. *Bioinformatics.* 2005;21(22):4187–9.
- Seo SW, Kim D, O'Brien EJ, Szubin R, Palsson BO. Decoding genome-wide GadEWX-transcriptional regulatory networks reveals multifaceted cellular responses to acid stress in *Escherichia coli*. *Nat Commun.* 2015;6:7970.
- Ma Z, Richard H, Tucker DL, Conway T, Foster JW. Collaborative regulation of *Escherichia coli* Glutamate-Dependent Acid Resistance by two AraC-Like regulators, GadX and GadW (YhiW). *J Bacteriol.* 2002;184:7001–12.
- Zhang R, Huang Y, Li M, Wang L, Li B, Xia A, et al. High-throughput, microscopy-based screening and quantification of genetic elements. *mLife.* 2023;2(4):450–61.
- MiKsch G, Bettenworth F, Friehs K, Flaschel E. The sequence upstream of the –10 consensus sequence modulates the strength and induction time of stationary-phase promoters in *Escherichia coli*. *Appl Microbiol Biotechnol.* 2005;69:312–20.

49. Gao Y, Zhao Y. Self-processing of ribozyme-flanked RNAs into guide RNAs in vitro and in vivo for CRISPR-mediated genome editing. *J Integr Plant Biol*. 2014;56(4):343–9.
50. Vlková M, Morampalli BR, Silander OK. Efficiency of the synthetic self-splicing RiboJ ribozyme is robust to *cis*- and *trans*-changes in genetic background. *MicrobiologyOpen*. 2021;10:e1232.
51. Gao X, Jiang L, Zhu L, Xu Q-t, Xu X, Huang H. Tailoring of global transcription sigma D factor by random mutagenesis to improve *Escherichia coli* tolerance towards low-pHs. *J Biotechnol*. 2016;224:55–63.
52. Zhou Y. Effect of lysine fermentation liquor pH value on the adsorption of ion exchange resin. *Cereal Food Ind*. 2014;21(01):15–7.
53. Boland PJ. Majority Systems and the Condorcet Jury Theorem. *Stat*. 1989;38:181–9.
54. Alon U. *An Introduction to Systems Biology*. Chapman and Hall/CRC; 2006.
55. Zhang J, Zhang Y, Zhao B-h, Zhang K, Liang D, Wei J, et al. Effects of pH on AHL signal release and properties of ANAMMOX granules with different biomass densities. *Environ Sci-Wat Res*. 2019;5(10):1723–35.
56. Yates EA, Philipp B, Buckley CM, Atkinson S, Chhabra SR, Sockett RE, et al. N-Acylhomoserine lactones Undergo Lactonolysis in a pH-, Temperature-, and acyl chain length-dependent manner during growth of *Yersinia pseudotuberculosis* and *Pseudomonas aeruginosa*. *Infect Immun*. 2002;70:5635–46.
57. Rana S, Bhawal S, Kumari A, Kapila S, Kapila R. pH-dependent inhibition of AHL-mediated quorum sensing by cell-free supernatant of lactic acid bacteria in *Pseudomonas aeruginosa* PAO1. *Microb Pathog*. 2020;142:104105.
58. Lutz RD, Bujard HPD. Independent and tight regulation of transcriptional units in *Escherichia coli* via the LacR/O, the TetR/O and AraC/I1-I2 regulatory elements. *Nucleic Acids Res*. 1997;25(6):1203–10.
59. Mutalik VK, Guimaraes JC, Cambray G, Lam C, Christoffersen MJ, Mai Q-A, et al. Precise and reliable gene expression via standard transcription and translation initiation elements. *Nat Methods*. 2013;10:354–60.
60. Gibson DG, Young L, Chuang R-Y, Venter JC, Hutchison CA III, Smith HO. Enzymatic assembly of DNA molecules up to several hundred kilobases. *Nat Methods*. 2009;6(5):343–5.
61. Zhang H, Lin M, Shi H, Ji W, Huang L, Zhang X, et al. Programming a pavlovian-like conditioning circuit in *Escherichia coli*. *Nat Commun*. 2014;5:3102.
62. Avis JM, Conn GL, Walker SC. *Cis*-acting ribozymes for the production of RNA in vitro transcripts with defined 5' and 3' ends. *Methods Mol Biol*. 2012;941:83–98.
63. Ying H, He X, Li Y, Chen K, Ouyang P. Optimization of culture conditions for enhanced lysine production using engineered *Escherichia coli*. *Appl Biochem Biotechnol*. 2014;172(8):3835–43.

Publisher's note

Springer Nature remains neutral with regard to jurisdictional claims in published maps and institutional affiliations.